

# Single phase $\text{In}_x\text{Ga}_{1-x}\text{N}$ ( $0.25 \leq x \leq 0.63$ ) alloys synthesized by metal organic chemical vapor deposition

B. N. Pantha,<sup>1</sup> J. Li,<sup>1</sup> J. Y. Lin,<sup>2</sup> and H. X. Jiang<sup>2,a)</sup>

<sup>1</sup>Department of Physics, Kansas State University, Manhattan, Kansas 66506-2601, USA

<sup>2</sup>Nano-Tech Center and Department of Electrical & Computer Engineering, Texas Tech University, Lubbock, Texas 79409, USA

(Received 18 September 2008; accepted 2 October 2008; published online 6 November 2008)

We present the results of single phase  $\text{In}_x\text{Ga}_{1-x}\text{N}$  alloys for the In composition ranging from 25% to 63% synthesized by metal organic chemical vapor deposition. Single peak of x-ray diffraction  $\theta$ - $2\theta$  scans of the (002) plane in InGaN alloys confirms that there is no phase separation. It was found both electron mobility and concentration increase with an increase of In content. Atomic force microscopy measurements revealed that the grown films have a surface roughness that varies between 1.5 and 4.0 nm and are free from In droplets. The results suggest that it is possible to synthesize single phase InGaN alloys inside the theoretically predicted miscibility gap. © 2008 American Institute of Physics. [DOI: 10.1063/1.3006432]

InGaN ternary alloy is of great interest because of its ability to tune the direct band gap from the near infrared region of  $\sim 0.7$  eV (InN) to the near UV region of  $\sim 3.4$  eV (GaN).<sup>1-4</sup> In particular, high quality In-rich InGaN alloys offer potential applications in many important areas including (1) whole solar spectrum, high efficiency, and radiation hard multijunction solar cells,<sup>5</sup> (2) high efficiency photoelectrochemical cells,<sup>6,7</sup> and (3) high brightness nitride green light emitting diodes and laser diodes.<sup>1</sup> More recently, our group showed that high In-content InGaN alloys are potentially important thermoelectric material for power generation and/or solid-state cooling.<sup>8</sup> These findings have further broaden the applications of ternary InGaN alloys into new areas that are distinctively different from traditional optoelectronics ones.

Many previous experimental studies have shown that the growth of high quality In-rich InGaN is extremely challenging due the low solubility of InN (GaN) in GaN (InN) (solid phase miscibility gap that usually results in phase separation in InGaN). Phase separation in InGaN has been theoretically predicted and experimentally observed.<sup>9-13</sup> However, so far the issue of phase separation is still under debate. Ho and Stingfellow's<sup>11</sup> calculation showed that the solubility of InN in GaN is only about 6% at the highest growth temperature and the miscibility gap covers almost the entire composition range. On the other hand, Karpov's<sup>14</sup> calculation revealed that phase separation may be considerably suppressed if the strain produced during the epitaxial process is taking into account; however, the problem remains significant for In content higher than 40%. The calculation also implied a much lower critical temperature and increased solubility in the strained InGaN alloys (750 °C versus 1175 °C and 6% versus 35%) compared to the previous calculation results in Ref. 11. This could be one of the reasons that InGaN alloys with InN fraction up to 30% (inside the miscibility gap from Ref. 11) without phase separation has been repeatedly grown by several techniques.<sup>9,10,15,16</sup> In a previous work, it was shown that single phase  $\text{In}_x\text{Ga}_{1-x}\text{N}$  films of  $x=0.5$  to 1 can be grown by metal organic chemical vapor deposition

(MOCVD) by lowering the growth temperature to 550 °C.<sup>17</sup> More recently, InGaN alloys (nanowires) without phase separation have been grown by molecular beam epitaxy/low pressure halide phase epitaxy in the entire composition range.<sup>18,19</sup> Here we present the growth and characterization of  $\text{In}_x\text{Ga}_{1-x}\text{N}$  alloys inside the previously thought phase separation regime by MOCVD.

$\text{In}_x\text{Ga}_{1-x}\text{N}$  alloys of thickness  $\sim 200$  nm with different InN fraction were grown on GaN/ $\text{Al}_2\text{O}_3$  and AlN/ $\text{Al}_2\text{O}_3$  templates by MOCVD. The precursors were trimethylgallium, trimethylindium, and ammonia ( $\text{NH}_3$ ) for Ga, In, and N, respectively. The growth pressure was 100 torr. The In content was controlled by growth temperature. In order to increase the In content from 25% to 63%, the growth temperature was decreased from 730 to 610 °C, while keeping all other conditions the same. GaN/ $\text{Al}_2\text{O}_3$  or AlN/ $\text{Al}_2\text{O}_3$  epitemplates were preheated in  $\text{NH}_3$  environment prior to the growth. There were no intermediate or buffer layers between the epitemplate and InGaN epilayer. In content in InGaN was estimated from peak value of x-ray diffraction (XRD) spectra of (002) reflection peak in  $\theta$ - $2\theta$  scan mode and applying Vegard's law. The thicknesses of the films were obtained from *in situ* interference measurements during the epigrowth. Electrical properties and surface morphology were probed by Hall-effect and atomic force microscopy (AFM) measurements.

Figures 1(a) and 1(b) show the XRD (002)  $\theta$ - $2\theta$  spectra of  $\text{In}_x\text{Ga}_{1-x}\text{N}$  alloys grown on GaN/ $\text{Al}_2\text{O}_3$  templates in linear and log scale, respectively. All curves, scanned down to InN peak position, have no multiple peaks, as seen by other authors with lower In content ( $<30\%$ ),<sup>9,10</sup> implies that InGaN alloys are not phase separated. The attainment of single phase InGaN alloys inside the previously thought miscibility gap by MOCVD here may be attributed to: 1) the presence of strain between the InGaN thin film and the epitemplate since we grew InGaN directly on the template without any buffer or intermediate layer to release it. 2) nonequilibrium growth processes taking place in epitaxial growth techniques like MOCVD, and 3) relatively low growth temperatures. This is, in fact, consistent with theoretical study of spinodal decomposition in strained InGaN by Karpov.<sup>14</sup> The inset of Fig. 1

<sup>a)</sup>Electronic mail: hx.jiang@ttu.edu.

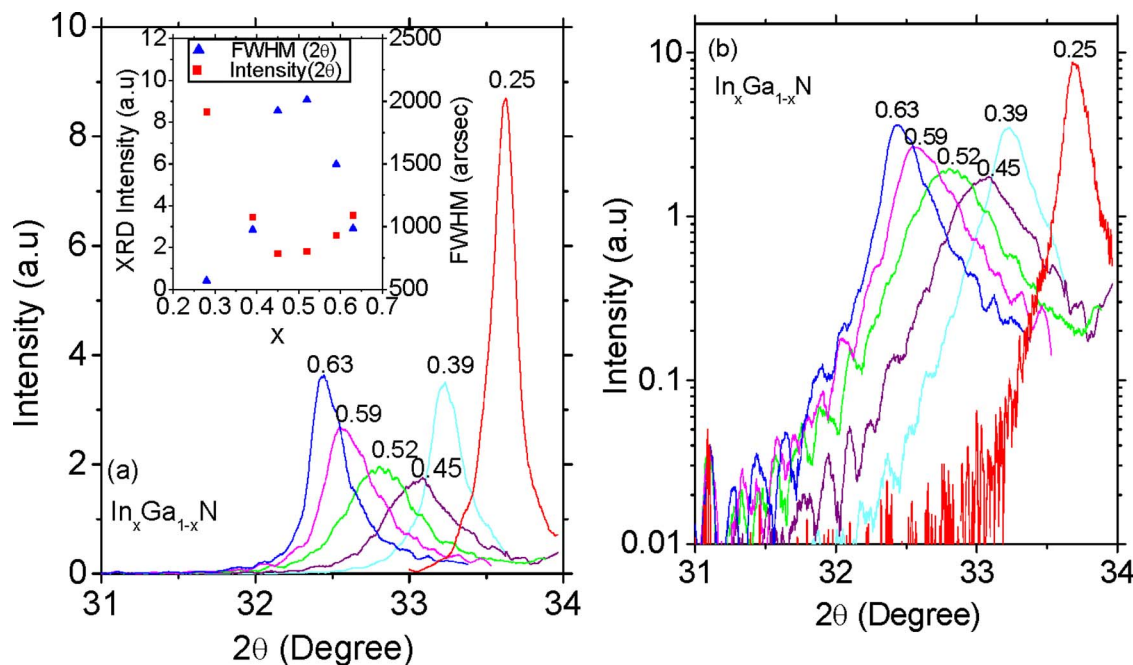


FIG. 1. (Color online) XRD  $\theta$ - $2\theta$  curves of (002) planes of  $\text{In}_x\text{Ga}_{1-x}\text{N}$  grown on GaN/ $\text{Al}_2\text{O}_3$  templates (a) in linear scale (b) in log scale. The inset shows the FWHMs and relative intensities as functions of In content.

shows the intensity and full width at half maximum (FWHM) of  $\theta$ - $2\theta$  curves as functions of In content in InGaN alloys. The FWHM is found to be varied between  $\sim 570$  and 2000 arc sec and correlated with the intensity. The higher the XRD intensity the smaller is the FWHM and vice versa. The FWHM of the  $\theta$ - $2\theta$  curves depends on many factors, including the homogeneity of the solid solution. We found that the homogeneity is quite good except the region where In content lies between 45% and 55%.

XRD (002) rocking curves of InGaN alloys and the variation in rocking curve FWHM with In content in InGaN are shown in Figs. 2(a) and 2(b), respectively. Figure 2(b) shows that FWHM increases as In content increases. Broadening of FWHM of rocking curves with In content is due to the increased lattice mismatch with GaN. We also found that the FWHM decreases as the thickness of InGaN layer decreases. The smallest value of FWHM of XRD (002) rocking curve was found to be associated with  $\text{In}_{0.45}\text{Ga}_{0.55}\text{N}$  alloy ( $\sim 60$  nm thick), which is about 600 arc sec with optimized growth conditions.

In content and growth rate of InGaN alloys as functions of growth temperature are shown in Fig. 3. Both the growth rate and In content increase linearly as the growth tempera-

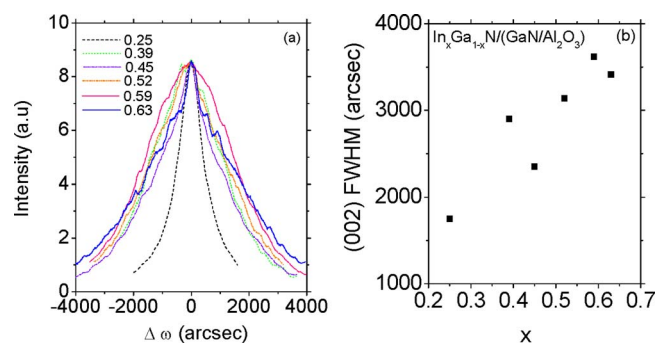


FIG. 2. (Color online) (a) XRD (002) rocking curves and (b) variation of FWHMs as functions of In content in  $\text{In}_x\text{Ga}_{1-x}\text{N}$  alloys.

ture decreases. The linear relation between the growth temperature and amount of In incorporation eases us to engineer the InGaN/GaN heterostructure for device applications. We also observed that In-incorporation can be increased by increasing growth rate, growth pressure, and flow rate of TMIn but the effectiveness of these parameters is found to be less pronounced as compared to the growth temperature.

Figure 4(a) shows the AFM images of  $\text{In}_x\text{Ga}_{1-x}\text{N}$  alloys grown on GaN/ $\text{Al}_2\text{O}_3$  templates for  $0.25 \leq x \leq 0.63$  with scanning area  $10 \times 10 \mu\text{m}^2$ . The surface roughness, quantified by the root-mean-square (rms) values, against the In content is plotted in Fig. 4(b). It was found that rms increases from 1.5 to 4.0 nm as  $x$  increases from 0.25 to 0.59. No indium droplets on the surface were observed in any samples we examined. We found similar surface morphologies of samples grown on AlN/ $\text{Al}_2\text{O}_3$  templates as well.

In order to evaluate the electrical properties, we grew InGaN alloys on AlN/ $\text{Al}_2\text{O}_3$  templates. These structures

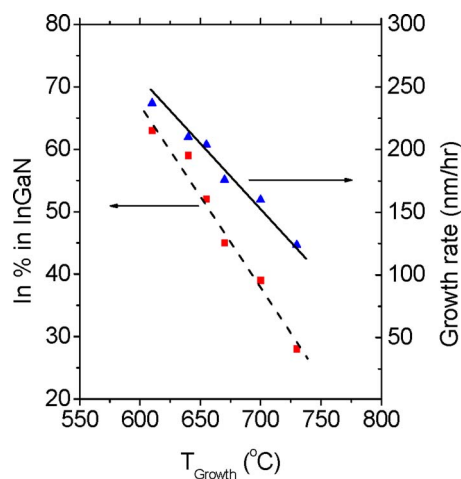


FIG. 3. (Color online) Growth rate and In content in  $\text{In}_x\text{Ga}_{1-x}\text{N}$  alloys as functions of growth temperature  $T_{\text{growth}}$ .

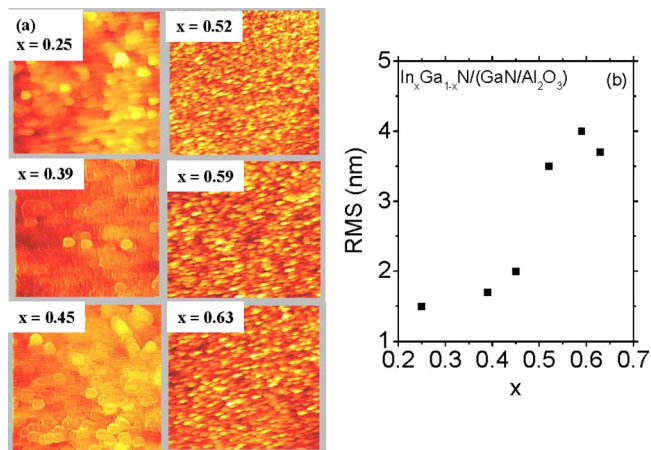


FIG. 4. (Color online) (a) AFM images and (b) Surface roughness (rms) as functions of In content in  $\text{In}_x\text{Ga}_{1-x}\text{N}$  alloys.

make the electrical measurement straightforward, quick, and precise because  $\text{AlN}$  is highly insulating. Compositional dependence of Hall mobility ( $\mu$ ) and free electron concentration ( $n$ ) of  $\text{InGaN}$  alloys with In content are plotted in Fig. 5. It is observed that both  $\mu$  and  $n$  increase as In content increases and  $n$  lies between  $(1.9\text{--}3.4) \times 10^{19} \text{ cm}^{-3}$  while  $\mu$  increases sharply as In mole fraction increases from 0.25 to 0.55. The reason for increasing  $\mu$  with increasing In content could be the lower effective mass of the electrons. The room

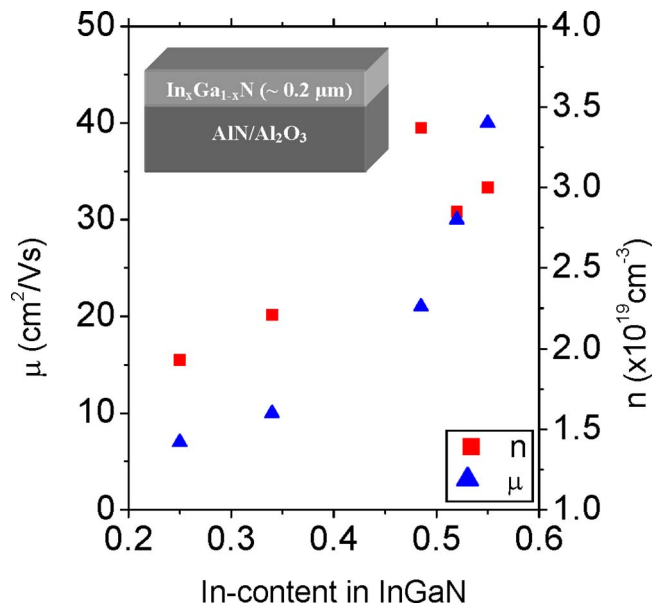


FIG. 5. (Color online) Hall mobility and electron concentration as functions of In content in  $\text{In}_x\text{Ga}_{1-x}\text{N}$  alloys. The layer structure employed for this study is shown in the inset.

temperature electron mobility of  $\text{In}_{0.55}\text{Ga}_{0.45}\text{N}$  alloys is about  $40 \text{ cm}^2/\text{V s}$  and pure  $\text{InN}$  is as high as  $1400 \text{ cm}^2/\text{V s}$ .<sup>20</sup>

In conclusion, we have synthesized  $\text{InGaN}$  alloys without phase separation inside the previously thought miscibility gap by MOCVD. We believe that the presence of strain, nonequilibrium nature of epitaxial growth process, and low growth temperatures have promoted the suppression of phase separation. The structural, electrical properties, and surface morphology studies indicated that  $\text{InGaN}$  alloys in this previously thought miscibility gap region possess reasonable good quality. Further improvement in material quality is expected by optimizing other growth parameters.

The  $\text{InGaN}$  epigrowth work is supported by NSF (DMR-0504601) and the material characterization work is supported by AFOSR (AF9550-06-1-0441). J.Y.L. and H.X.J. gratefully acknowledge the support of the Linda Whitacre and Edward Whitacre endowed chair positions through the AT&T Foundation.

<sup>1</sup>S. Nakamura and G. Fasol, *The Blue Laser Diode* (Springer, Berlin, 1997), pp. 201–260.

<sup>2</sup>J. Wu, W. Walukiewicz, K. M. Yu, J. W. Ager III, E. E. Haller, H. Lu, and W. J. Schaff, *Appl. Phys. Lett.* **80**, 4741 (2002).

<sup>3</sup>J. Wu, W. Walukiewicz, K. M. Yu, J. W. Ager III, E. E. Haller, H. Lu, W. J. Schaff, Y. Saito, and Y. Nanishi, *Appl. Phys. Lett.* **80**, 3967 (2002).

<sup>4</sup>V. Yu. Davydov, A. A. Klochikhin, R. P. Seisyan, and V. V. Emtsev, *Phys. Status Solidi B* **229**, R1 (2002).

<sup>5</sup>J. Wu, W. Walukiewicz, K. M. Yu, W. Shan, J. W. Ager III, E. E. Haller, H. Lu, W. J. Schaff, W. K. Metzger, and S. Kurtz, *J. Appl. Phys.* **94**, 6477 (2003).

<sup>6</sup>K. Fujii, K. Kusakabe, and K. Ohkawa, *Jpn. J. Appl. Phys., Part 1* **44**, 7433 (2005).

<sup>7</sup>O. Khaselev and J. A. Turner, *Science* **280**, 425 (1998).

<sup>8</sup>B. N. Pantha, R. Dahal, J. Li, J. Y. Lin, H. X. Jiang, and G. Pomrenke, *Appl. Phys. Lett.* **92**, 042112 (2008).

<sup>9</sup>N. A. El-Masry, E. L. Piner, S. X. Liu, and S. M. Bedair, *Appl. Phys. Lett.* **72**, 40 (1998).

<sup>10</sup>R. Singh, D. Doppalapudi, T. D. Moustakas, and L. T. Romano, *Appl. Phys. Lett.* **70**, 1089 (1997).

<sup>11</sup>I. Ho and G. B. Stringfellow, *Appl. Phys. Lett.* **69**, 2701 (1996).

<sup>12</sup>J. Adhikari and D. A. Kofke, *J. Appl. Phys.* **95**, 4500 (2004).

<sup>13</sup>L. K. Teles, M. Marque, L. M. R. Scolfaro, and J. R. Leite, *Braz. J. Phys.* **34**, 593 (2004).

<sup>14</sup>S. Y. Karpov, *MRS Internet J. Nitride Semicond. Res.* **3**, 16 (1998).

<sup>15</sup>H. P. D. Schenk, P. de Mierry, M. Laigt, F. Omnes, M. Leroux, B. Beaumont, and P. Gibart, *Appl. Phys. Lett.* **75**, 2587 (1999).

<sup>16</sup>M. Hori, K. Kano, T. Yamaguchi, Y. Satio, T. Araki, Y. Nanishi, N. Terauchi, and A. Suzuki, *Phys. Status Solidi B* **234**, 750 (2002).

<sup>17</sup>A. Yamamoto, Y. Nakagawa, T. Sugiura, and A. Hashimoto, *Phys. Status Solidi A* **176**, 237 (1999).

<sup>18</sup>E. Iliopoulos, A. Georgakilas, E. Dimakis, A. Adikimenakis, K. Tsagaraki, M. Androulidaki, and N. T. Pelekanos, *Phys. Status Solidi A* **203**, 102 (2006).

<sup>19</sup>T. Kuykendall, P. Ulrich, S. Aloni, and P. Yang, *Nature Mater.* **6**, 951 (2007).

<sup>20</sup>N. Khan, A. Sedhain, J. Li, J. Y. Lin, and H. X. Jiang, *Appl. Phys. Lett.* **92**, 172101 (2008).